Long-range carrier-mediated Cu-Cu interactions and low-temperature transitions in the quasi-one-dimensional Cu_xNi_{1-x}(phthalocyanine)I alloys

Michael Y. Ogawa, Sharon M. Palmer, and Kwangkyoung Liou
Department of Chemistry and Materials Research Center, Northwestern University, Evanston, Illinois 60201

Guy Quirion
Centre de Recherche en Physique du Solide, Département de Physique, Université de Sherbrooke, Sherbrooke, Quebec, Canada J1K 2R1

Julia A. Thompson
Department of Chemistry and Materials Research Center, Northwestern University, Evanston, Illinois 60201

Mario Poirier
Centre de Recherche en Physique du Solide, Département de Physique, Université de Sherbrooke, Sherbrooke, Quebec, Canada J1K 2R1

Brian M. Hoffman
Department of Chemistry and Materials Research Center, Northwestern University, Evanston, Illinois 60201
(Received 8 September 1988)

A series of alloys Cu_xNi_{1-x}(PC)I (PC = phthalocyanine) of the two isostructural molecular conductors, phthalocyaninato nickel(II) iodide, Ni(PC)I, and phthalocyaninato copper(II) iodide, Cu(PC)I, have been prepared. These crystals contain partially oxidized M(PC) stacks and are quasi-one-dimensional molecular metals whose charge carriers are associated with the highest occupied π molecular orbitals of the PC macrocycles. The Cu^{2+} ($S=\frac{1}{2}$) local moments of Cu_xNi_{1-x}(PC)I remain exchange coupled even when the paramagnetic metal-ion chain incorporated within the M(PC) stacks is diluted ($x \ll 1$) with the diamagnetic Ni^{2+} ions and the Cu magnetization is also coupled to the itinerant π-electron charge carriers. For alloys with $x \geq 0.1$, the EPR signal of the coupled magnetization exhibits two anomalies at low temperature. The g values and linewidths first begin to deviate from their high-temperature behavior at $T_a \sim 25$ K, roughly independent of composition for $0.05 \leq x < 1$. A more dramatic response of the linewidth occurs upon cooling through T_b, which decreases from ~ 8 K as x is reduced from 1.0. Surprisingly, the g value of the $x=0.50$ alloy at low temperature shows a field dependence: At X-band frequency, $g_{\|}$ increases to ~ 2.21 by $T \sim 2.3$ K, a g value much larger than that of the parent Cu(PC) ($g_{\|}=2.18$); this anomaly is quenched at a higher observing field (Q-band frequency). These alloys are highly conducting, as are the two parent materials. The dependence of the conductivity on x indicates that $\sigma(T)$ is governed by magnetic scattering by the Cu^{2+} ions. In the low-temperature region, the results for the four-probe and microwave conductivity differ sharply in a composition-dependent fashion and indicate a novel coupling between dielectric and magnetic properties.

INTRODUCTION

We report here the properties of alloys between the two isostructural porphyrinic molecular metals,[1] phthalocyaninato nickel(II) iodide, Ni(PC)I,[2] and phthalocyaninato copper(II) iodide, Cu(PC)I.[3,4] These two compounds crystallize as metal-over-metal stacks of partially ($\frac{1}{3}$) oxidized M(PC) units surrounded by chains of I_3^- counterions. Both are organic conductors whose charge carriers are associated with the highest occupied π molecular orbitals of the PC ring. For Ni(PC)I the Ni^{2+} ions are diamagnetic and play no direct role in the electronic or magnetic properties of the crystals.[2] However, Cu(PC)I is a novel material because its Cu^{2+} (d^9, $S=\frac{1}{2}$) ions are paramagnetic and form a linear magnetic chain embedded within a one-dimensional "Fermi sea" of organic charge carriers.[3]

The copper sites in Cu(PC)I are exchange coupled to one another as well as to the itinerant carriers. This unusual situation, found also in Cu(TATBP)I,[5] (TATBP is triazatetrabenzporphyrinato) results in the observation of a new type of low-temperature phenomenon characterized by transitions of the coupled local-moment–itinerant-carrier systems. These include the onset of anomalies in the EPR g shift and linewidth at $T_a \sim 20$ K, and an abrupt broadening and disappearance of the EPR signal at $T_b \sim 8$ K that occurs without an associated loss of paramagnetism.[6] The T_b transition is accompanied by unusual features in the microwave conductivity,[7] and ^{1}H NMR spin-lattice-relaxation times.[6] The Cu^{2+} spin sys-

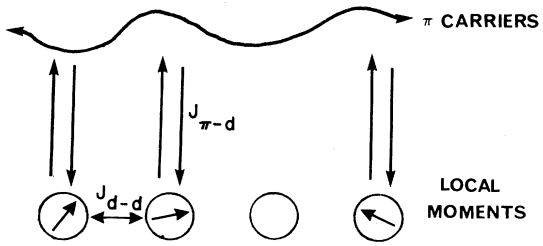

FIG. 1. Representation of one-dimensional exchange interactions of Cu^{2+} ($S=\frac{1}{2}$) spins (circles with arrows) with neighbors ($J_{d\text{-}d}$) and with carriers ($J_{\pi\text{-}d}$). Diamagnetic Ni^{2+} ion ($S=0$) is indicated by an open circle.

tem dominates the magnetic properties of Cu(PC)I at low temperatures, and these low-temperature transitions may well be driven by the Cu^{2+} paramagnets. Analysis of the NMR relaxation times indicated that *direct* exchange coupling between neighboring Cu^{2+} sites is small ($J_{\rm dir}/k_B \approx 0.3$ K) as compared to the total exchange energy estimated from the Curie-Weiss temperature or EPR-linewidth data ($J/k_B \approx 6$ K).[5] It was therefore suggested that direct interactions between neighboring Cu^{2+} sites do not play a significant role in the low-temperature behavior of Cu(PC)I and that long-range, carrier-mediated interactions between copper spins predominate.

To further characterize this novel situation and to test the hypothesis that *indirect* Cu-Cu interactions drive the EPR transition in Cu(PC)I, we have prepared a homologous series of compounds, Cu_xNi_{1-x}(PC)I, having a wide range of local moment, Cu^{2+}, concentration, $0.05 \leq x \leq 1.0$. These compounds are shown to be solid solutions and can be considered as alloys of the molecular metals, Cu(PC)I and Ni(PC)I, in which direct Cu-Cu exchange is interrupted by intervening diamagnetic Ni(PC) sites (Fig. 1). The Cu^{2+} local moments of Cu_xNi_{1-x}(PC)I remain exchange coupled even when diluted ($x \ll 1$) and the Cu magnetization also is coupled to the itinerant π-electron charge carriers. At low temperatures, the coupled EPR signal of materials with $x \geq 0.1$ exhibits anomalies related to the two observed for Cu(PC)I and Cu(TATBP)I. These studies support the hypothesis that the π carriers mediate long-range, indirect interactions between the Cu^{2+} spins, and that these interactions are fundamental to the low-temperature transition first observed in Cu(PC)I.

EXPERIMENT

Synthesis of Cu_xNi_{1-x}(PC)I

Copper and nickel phthalocyanine [Cu(PC) and Ni(PC)] were purchased from the Eastman Kodak Company and sublimed two or three times prior to further use (400 °C at 10^{-3} Torr). The purified materials were ground together in the desired proportions, and the resulting mixtures were sublimed to yield red-violet crystals of Cu_xNi_{1-x}(PC). This procedure was consistently found to result in an even distribution of paramagnetic Cu(PC) and diamagnetic Ni(PC) molecules in both these nonconductive materials and in their conductive counterparts (*vide infra*).

Cu_xNi_{1-x}(PC)I was prepared as follows. Solid Cu_xNi_{1-x}(PC) of the appropriate composition was placed in one arm of an H tube, and excess I_2 was added to the other arm with 1-chloronaphthalene as a solvent. The side containing the M(PC) was heated to ca. 170 °C, hotter than was used to prepare the Cu(PC)I studied in Ref. 3. After several days, large (2–3 mm) green-black needles of Cu_xNi_{1-x}(PC)I were obtained from the cooler portion of the tube. In the case of $x=0.75$, the reaction did not produce homogeneous bulk material. Instead, single crystals of $Cu_{0.75}Ni_{0.25}$(PC)I were found to be mixed with crystals of the unoxidized starting material; individual crystals of the former material were easily separated under a binocular microscope.

Elemental analyses (C, H, and N analysis; Microtech Laboratories, Inc., Skokie, II) were performed on samples prepared to have the composition, Cu_xNi_{1-x}(PC)I ($x=0.05$, 0.10, 0.25, and 0.50). They confirm that each material has the stoichiometry, M(PC)I, with one iodine atom per macrocycle. The same is assumed for $Cu_{0.75}Ni_{0.25}$(PC)I; no analysis was performed for this composition as there was not sufficient bulk material. Analyses for Cu_xNi_{1-x}(PC)I were as follows. For $x=0.05$: Calculated C, 55.03; H, 2.31; N, 16.04. Found C, 55.15; H, 2.39; N, 16.10. For $x=0.10$: C, 55.02; H, 2.31; N, 16.04. Found C, 55.09; H, 2.45; N, 16.18. For $x=0.25$: C, 54.96; H, 2.48; N, 16.06. Found C, 54.82; H, 2.48; N, 16.06. For $x=0.50$: C, 54.68; H, 2.31; N, 15.99. Found C, 54.74; H, 2.34; N, 15.79.

Resonance Raman measurements

Raman-spectra measurements were made at ambient temperature on polycrystalline samples of Cu_xNi_{1-x}(PC)I contained in 5-mm Pyrex types. The tubes were spun ($\sim$1200 rpm) to eliminate decomposition of the sample by the laser. The spectra were recorded on a spectrometer described elsewhere[8] using a 5145-Å Ar^+ laser line as the excitation source and were corrected, where necessary, for the plasma line.

Magnetic susceptibility measurements

Static magnetic susceptibility measurements were obtained using a VTS Model 50 susceptometer at an external field of either 5 or 10 kG within the temperature range $300 \geq T \geq 1.7$ K. The paramagnetic component of the observed susceptibilities of Cu_xNi_{1-x}(PC)I were obtained by correcting for the core diamagnetism of triiodide, the PC ring, and the metal center using Pascal's constants, as previously.[2] Samples, consisting of 20–30 mg of polycrystalline materials, were crushed to avoid anisotropy effects and placed in sample holders made of high-purity spectrosil quartz (Thermal American, Inc. NJ). A background calibration of the sample holder was routinely run over the full temperature range just prior to each experiment. Calibration of the instrument was

checked with a Pd standard obtained from the National Bureau of Standards.

Electron paramagnetic resonance measurements

EPR spectra at *X*-band frequencies (~ 9 GHz) were obtained as described earlier.[2,3] Single-crystal spectra were obtainable from Cu_xNi_{1-x}(PC)I for $x = 0.75$, 0.50, and 0.25; the signals from single crystals of samples with $x = 0.10$ and 0.05 were sufficiently weak that powdered samples were employed for temperatures above 100 K. EPR measurements at $T \leq 4.2$ K employed powder samples and a pumped-helium immersion cryostat; similar samples and procedures were used for *X*-band and *Q*-band (~ 35 GHz) measurements. Simulations of powder spectra were used to determine the *g* values and linewidths.[9]

Conductivity

Single-crystal conductivities were measured with a four-probe (27 Hz) apparatus previously described.[2] A standard microwave cavity perturbation technique[10] was used to measure the 17 GHz conductivity and the dielectric constant.

Electron microanalytical probe

Electron-microprobe analysis was performed on a Cambridge Scientific Instruments, Ltd., Stereoscan S-4 Scanning electron microscope.

RESULTS

Characterization of Cu_xNi_{1-x}(PC)I

To compare the properties of Cu_xNi_{1-x}(PC)I with those of Cu(PC)I, it is necessary to establish the stoichiometry of these materials and to prove that they exist as homogeneous solid solutions and not segregated regions of Cu(PC)I and Ni(PC)I. The C,H,N analyses listed in the Experimental section confirm that each prepared material has a composition corresponding to one iodine atom per macrocycle but cannot accurately determine the relative amounts of Cu and Ni, namely, the value of *x* in Cu_xNi_{1-x}(PC)I. This was accurately determined by magnetic-susceptibility measurements described below. Electron-microprobe analysis confirmed these susceptibility results and demonstrated that the Cu and Ni are homogeneously distributed on a macroscopic (≥ 1 μm) scale. Finally, EPR measurements performed on samples that had been deiodinated to give Cu_xNi_{1-x}(PC) indicate that the Cu(PC) and Ni(PC) molecules in Cu_xNi_{1-x}(PC)I are homogeneously distributed on a microscopic, molecular level.

Resonance Raman spectroscopy

The resonance Raman spectra of polycrystalline samples of Cu_xNi_{1-x}(PC)I at room temperature are identical over the entire range, $0.05 \leq x \leq 1.0$. Each exhibits a sharp fundamental peak at 107 cm^{-1}, with overtone peaks occurring at 213, 320, and 436 cm^{-1}. This pattern is characteristic of linear chains of symmetrical triiodide ions.[11] The absence of any observable peaks having an intensity larger than that of the overtone band at either 167 or 212 cm^{-1} eliminates I_5^- or I_2 as being significant iodine forms in these materials. By analogy with the study of Ni(PC)I[2a] for which ^{129}I Mössbauer experiments provided no evidence for the presence of I^-, we conclude that the same holds for Cu_xNi_{1-x}(PC)I. Thus, the Cu_xNi_{1-x}(PC)I can be described formally with the mixed-valence notation, $[Cu_xNi_{1-x}(PC)]^{0.33+}[I_3^-]_{0.33}$, to indicate partial oxidation of one-third of the electrons per metallomacrocycle.

Magnetic-susceptibility measurements

Room-temperature magnetic-susceptibility measurements were used to determine the fraction of the paramagnetic Cu^{2+} ($S = \frac{1}{2}$) ions in Cu_xNi_{1-x}(PC)I. Samples of each composition, *x*, were first quantitatively deiodinated by heating overnight to 160 °C *in vacuo* (10^{-3} Torr). The paramagnetic susceptibility of the resulting Cu_xNi_{1-x}(PC) was obtained by correcting for the suscep-

TABLE I. Composition and magnetic susceptibility data for Cu_xNi_{1-x}(PC)I.

x (in reagents)	x^{a-c} (measured)	C_{obs}[a] (emu K mol^{-1})	χ_π[a] (emu mol^{-1})	Θ[a] (K)
1.0[d]	0.98	0.394	1.9×10^{-4}	−4.0
0.50	0.57	0.2304	1.4×10^{-4}	−2.47
0.25	0.28	0.1137	1.6×10^{-4}	−1.59
0.10	0.09	0.0351	3.0×10^{-4}	−0.83
0.05	0.06	0.0226	3.1×10^{-4}	−0.069

[a]Susceptibility for Cu_xNi_{1-x}(PC)I was fit to Eq. (1). To best characterize the behavior of the local-moment spin system, values presented in this table are determined by fitting the data within the temperature range $10 \leq T \leq 100$ K to Eq. (2).

[b]As described in the text, *x* is measured by fitting the susceptibility of the deiodinated material to the Curie-law formula: $x = C_{obs}/C_{calc}$, where $C_{calc} = Ng^2\mu_B^2 S(S+1)/sk_B = 0.409$ emu K mol^{-1}.

[c]To best characterize the behavior of the local-moment spin systems, values presented in this table are determined by fitting the data within the temperature range $10 \leq T \leq 100$ K to Eq. (2).

[d]Reference 3.

tibility of the sample holder and the core diamagnetism of the sample as estimated from Pascal's constants. As these materials are insulators and there is no contribution from charge carriers, the stoichiometric coefficient x of Cu_xNi_{1-x}(PC), and thus of Cu_xNi_{1-x}(PC)I was calculated from the paramagnetic susceptibility through use of the Curie-law formula

$$\chi_p = C_{obs}/T = xC_0 T \ . \quad (1)$$

Here C_0 is the calculated Curie constant for one Cu^{2+} spin per site: $C_0 = Ng^2\mu_B^2 S(S+1)/3k_B = 0.409$, where N is Avogadro's number, μ_B is the Bohr magneton, k_B is Boltzmann's constant, $S = \frac{1}{2}$, $g^2 = \frac{1}{3}(2g_\perp^2 + g_\parallel^2) = 4.367$ as calculated from the EPR g values of polycrystalline Cu(PC).[4] Results presented elsewhere show that it is not necessary to use the more general Curie-Weiss formula for this analysis because the Weiss constant for interactions between Cu^{2+} spins in these materials has a negligible influence at this temperature; for Cu(PC),[4] $\Theta = -0.11$ K. The susceptibility results presented in Table I demonstrate that the compositional variable, x, in Cu_xNi_{1-x}(PC)I as measured in this way is in good agreement with the Cu:Ni ratios of the starting materials used in the initial iodination reaction.

Electron microprobe

Semiquantitative analyses by electron microprobe were performed on single crystals of Cu_xNi_{1-x}(PC)I to confirm the relative amounts of Cu and Ni. In each case, the atomic ratio of Cu:Ni was approximately equal to the original ratio of Cu(PC):Ni(PC) in the starting mixture. In the electron-microprobe experiments, the electron beam also was traversed along the length and breadth of individual crystal faces. These experiments demonstrate that the distribution of Cu and Ni within crystals of Cu_xNi_{1-x}(PC)I is homogeneous on the scale determined by the size of the electron beam ($\gtrsim 1$ μm diameter).

Microscopic distribution of Cu(PC) and Ni(PC) sites by EPR

To examine the microscopic distribution of Cu(PC) and Ni(PC) sites in Cu_xNi_{1-x}(PC)I, EPR measurements were again conducted on deiodinated samples of Cu_xNi_{1-x}(PC), because their magnetic properties are not complicated by the presence of mobile charge carriers. The deiodination procedure was conducted *in vacuo* (10^{-3} Torr) at temperatures of ~ 160 °C, substantially below the sublimation point of metallophthalocyanines ($T_{sub} \approx 400$ °C, 10^{-3} Torr). Thus, molecular migration will not occur during this procedure and the distribution of the component molecules in the deiodinated samples will reflect that for the conductive materials.

Figure 2 presents the room-temperature EPR spectra of polycrystalline samples of Cu_xNi_{1-x}(PC), $x = 1.0$, 0.25, and 0.10, prepared in the above fashion. The EPR parameters of the isolated Cu(PC) molecule have been previously studied in magnetically dilute single crystals.[12] Its g tensor has the principal values $g_\parallel = 2.179$ and $g_\perp = 2.050$, and large hyperfine couplings to the Cu center may be observed in addition to smaller couplings to the coordinating N atoms. In the absence of intermolecular magnetic interactions, the EPR spectrum of polycrystalline Cu(PC) is expected to exhibit an axially symmetric EPR signal having clearly resolved Cu and N hyperfine features. However, as seen in Fig. 2, the observed EPR signal of polycrystalline Cu(PC) displays poorly resolved axial symmetry without evidence for hyperfine coupling to either ^{63,65}Cu or ^{14}N. This is as expected from a previous study[4] in which Cu(PC) was shown to behave as a highly-one-dimensional Heisenberg antiferromagnet. The dipolar interactions between neighboring Cu^{2+} sites gives the EPR line a second moment of $M_2 = 2.5 \times 10^4$ G^2, which would correspond to an EPR linewidth of $(M_2)^{1/2} \approx 500$ G; exchange coupling, $|J/k_B| \lesssim 0.3$ K, between near-neighbor Cu^{2+} sites narrows this dipolar width to produce the observed spectrum.

If the Cu and Ni sites of Cu_xNi_{1-x}(PC)I existed in segregated domains, then the EPR of deiodinated Cu_xNi_{1-x}(PC) would be similar to that of Cu(PC) for all x, merely reduced in intensity by a factor of x. This clearly is not the case (Fig. 2). These results extend the conclusions based on the electron microprobe analysis and indicate that the two types of M(PC) are microscopically dispersed within the Cu_xNi_{1-x}(PC)I.

At high values of x, the use of EPR methods to characterize the microscopic dispersion of Cu and Ni sites in Cu_xNi_{1-x}(PC) is complicated by two competing effects. First, lowering the concentration of paramagnetic spins by the introduction of diamagnetic Ni(PC) molecules tend to *narrow* the EPR line as this reduces the dipolar interactions between neighboring Cu^{2+} sites; in the limit of a randomly diluted system, $M_2(x) = xM_2(1)$ where

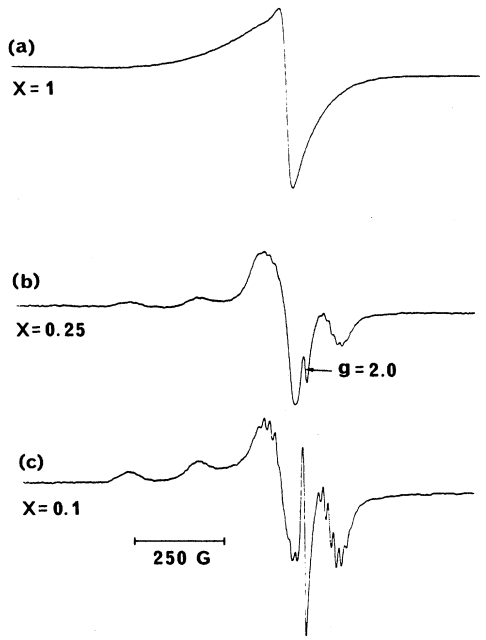

FIG. 2. Powder EPR spectra of deiodinated samples of Cu_xNi_{1-x}(PC) with $x = 1.0$, 0.25, and 0.10.

$M_2(1)$ is the dipolar second moment of the magnetically condensed material.[13] Secondly, the interruption of the one-dimensional Cu(PC) chain by intervening Ni(PC) molecules will reduce the effects of exchange, thereby tending to *broaden* the EPR line. The spectrum at $x=0.50$ (not shown) clearly demonstrates these effects: it may be described as the superposition of a narrow signal arising from groups of Cu(PC) molecules, where the sharpening effects lead to a well-resolved, but exchange-narrowed, feature at $g_\perp=2.05$, and of a broad EPR line dominated by dipolar interactions.

At lower values of x, the situation becomes simpler. The small exchange interaction present within the M(PC) structure ($|J/k_B|<0.3$ K) would have no measurable effect upon the EPR of small oligomers of Cu(PC) molecules and thus, only dipolar-broadening effects should be observed.[14] As seen in Fig. 2, the Cu hyperfine splittings are indeed well resolved by $x=0.25$, and the hyperfine coupling constants are those of the isolated molecule. By $x=0.10$, the spectrum is better resolved and evidence for ^{14}N splitting is now detectable. For $x=0.05$, the spectrum approaches that of an isolated Cu(PC) molecule. This smooth progression of spectra features observed as x decreases from ~ 0.50 strongly suggests that the distribution of Cu(PC) and Ni(PC) molecules in Cu_xNi_{1-x}(PC)I is essentially homogeneous on the molecular level.

In summary, electron microprobe analysis of Cu_xNi_{1-x}(PC)I and EPR studies of deiodinated samples of this material show no evidence for the segregation of Cu and Ni complexes in Cu_xNi_{1-x}(PC)I sites on either the macroscopic or molecular scales. Thus, we shall treat the Cu_xNi_{1-x}(PC)I as true solid solutions of the constituent molecular subunits. As the two parent compounds Cu(PC)I and Ni(PC)I each behaves as a molecular metal,[2,3] we may consider these solutions as molecular alloys.

Properties of Cu_xNi_{1-x}(PC)I

Magnetic-susceptibility measurements

Susceptibility measurements provide a convenient probe to examine the magnetic interactions present in Cu_xNi_{1-x}(PC)I. The temperature dependence of the static paramagnetic susceptibility for Cu(PC)I, $x=1.0$, has been reported[3] and Fig. 3 presents χ^{-1} as a function of temperature for compounds with $x\leq 0.50$. Measurements for bulk samples, $0.5<x<1.0$, could not be performed as only small quantities of single crystals were available. For all compositions studied, the observed susceptibilities increase with decreasing temperature and for $T\gtrsim 10$ K accurately follow an expression that contains a Curie-Weiss contribution associated with a system of localized magnetic moments and a temperature independent, Pauli-like component associated with charge carriers

$$\chi(T)=\chi_{Cu}(T)+\chi_P$$
$$=C_{obs}/(T-\Theta)+\chi_P\ . \qquad (2)$$

To best characterize the magnetic behavior of the local spin system of these materials, we have analyzed the susceptibility data for $10\leq T\leq 100$ K, where the Curie-Weiss contribution dominates. As shown in Fig. 3, the data within this temperature range fit Eq. (2) extremely well. Table I summarizes the results of this analysis. The observed Curie constant for Cu_xNi_{1-x}(PC)I is linearly dependent upon the fractional occupancy of Cu^{2+} ions: $C_{obs}(x)=xC_0$, where C_0 is the calculated Curie constant for pure Cu(PC)I. Thus, for all x, including $x=1$ [pure Cu(PC)I],[3] the local spin system in the Cu_xNi_{1-x}(PC)I is comprised of the paramagnetic Cu^{2+} spins, and the charge carriers are associated solely with the π orbitals of the PC ring. If the converse were true and the copper centers of these materials were partially oxidized, the resultant Curie constants would have been reduced from those that were observed. Examination of the Pauli contribution to the susceptibility of Cu_xNi_{1-x}(PC)I supports this conclusion, as these values are close to the observed for the $x=0$ organic conductor, Ni(PC)I[2c] ($\chi_P=2\times 10^{-4}$ emu mol^{-1}).

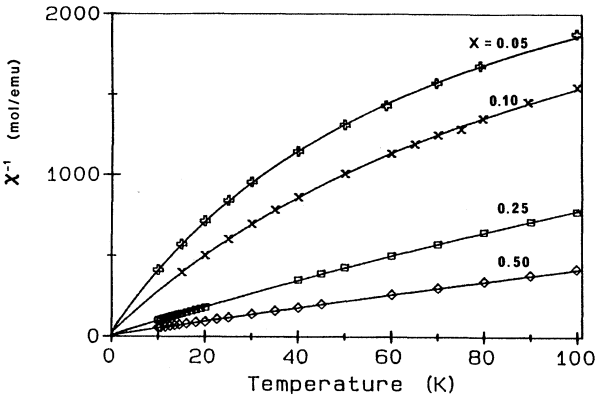

FIG. 3. Inverse, bulk paramagnetic susceptibility (mol/emu) of Cu_xNi_{1-x}(PC)I plotted as a function of temperature for $x=0.50$, 0.25, 0.10, and 0.05. The solid lines indicate the best fit of the data to Eq. (2) as described in the text.

The Weiss temperature Θ which provides a measure of the exchange interactions involving the paramagnetic Cu^{2+} sites, varies linearly with the concentration of Cu^{2+} sites in Cu_xNi_{1-x}(PC)I (Fig. 4). As discussed for Cu(PC)I,[3] the Weiss temperature for Cu_xNi_{1-x}(PC)I may have two separate contributions: $\Theta_{OBS}=\Theta_{dir}+\Theta_{ind}$. In a one-dimensional Cu^{2+} chain, direct, near-neighbor Heisenberg interactions between adjacent spins would give rise to a term, $\Theta_{dir}=|J_{nn}|/k_B$, where J_{nn} is the exchange parameter.[15] In the conductive Cu_xNi_{1-x}(PC)I a second term, Θ_{ind}, arises from an indirect, carrier-mediated exchange between distant Cu^{2+} neighbors.[16] This interaction is introduced because there is an intramolecular exchange interaction, $J_{d\text{-}\pi}$, between the localized spin associated with the in-plane $d_{x^2-y^2}$ orbital of the Cu^{2+} ion and the mobile charge carriers whose wave functions involve the highest occupied π orbitals of the PC ring;[17] a perturbation-theory approach would give $\Theta_{ind}\propto J^2_{d\text{-}\pi}$.

^{1}H NMR measurements indicate that direct exchange interactions between adjacent Cu^{2+} sites are weak in

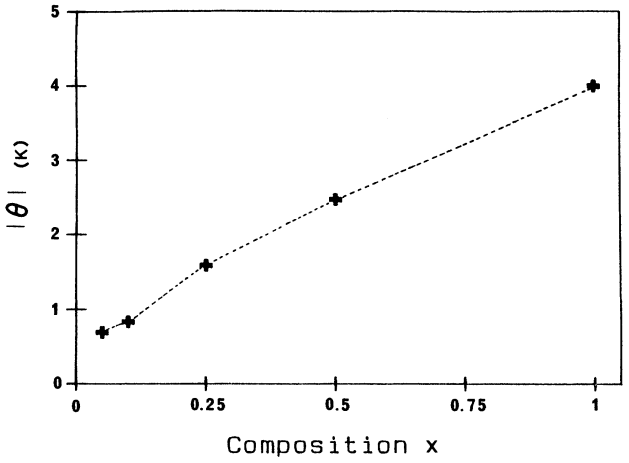

FIG. 4. Absolute value of the Weiss constants, Θ, for Cu_xNi_{1-x}(PC)I plotted as a function of composition (x).

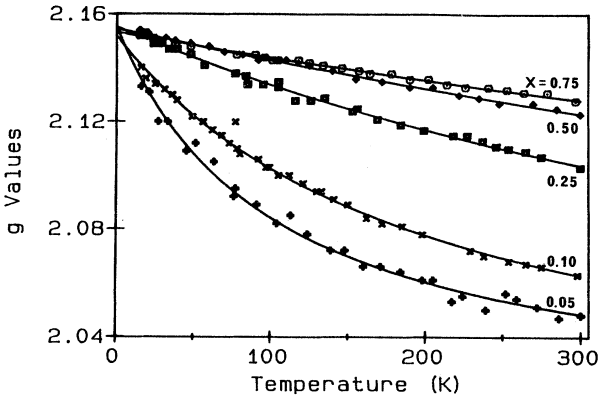

FIG. 5. Parallel component of the EPR g tensor of Cu_xNi_{1-x}(PC)I plotted as a function of temperature. The solid lines indicate the best fit of the data to Eq. (3) as described in the text.

Cu(PC)I, $|\Theta_{dir}| < 0.3$ K.[6] Such interactions would be further diminished in the Cu_xNi_{1-x}(PC)I by the incorporation of diamagnetic Ni^{2+} ions within the M(PC) spine and the effects of Θ_{dir} can be neglected in these materials. Thus, we infer that the indirect, carrier-mediated interactions dominate the exchange coupling between the Cu^{2+} spins in Cu_xNi_{1-x}(PC)I. It is expected that Θ_{ind} introduced by such couplings would vary linearly with the concentration of Cu^{2+} sites,[18] consistent with the results in Fig. 4.

EPR results: $T > 20$ K

g values

The EPR signal of Cu_xNi_{1-x}(PC)I consists of a single, roughly Lorentzian line whose g values and linewidth are angle and temperature dependent. The susceptibility data presented in the preceding section demonstrate that these alloys of Cu(PC)I and Ni(PC)I possess two distinct magnetic subsystems: an array of localized Cu^{2+} spins and mobile π-electron charge carriers. As with Cu(PC)I these mixed materials exhibit a *single* EPR line demonstrating the existence of exchange coupling $[J \gg (g^{Cu} - g^{\pi})\mu_B H_0]$ between the two magnetic systems. EPR measurements have been performed on single crystals of Cu_xNi_{1-x}(PC)I, where $x = 1.0, 0.75, 0.50$. Each composition exhibits an axially symmetric g tensor whose unique axis corresponds to the crystal-needle axis. For materials with $x \lesssim 0.25$, EPR signals from single crystals were too weak to be observed at temperatures greater than ~ 20 K, but powder EPR spectra show that they also display an axially symmetric g tensor, $g_{\parallel} > g_{\perp}$. As shown in Fig. 5, at any temperature above $T \sim 20$ K, the g values increase with increasing concentrations of Cu sites but remain intermediate between those expected for isolated Cu(PC) ($g_{\parallel} \sim 2.18$, $g_{\perp} = 2.05$) and π carrier spins ($g_{av} \approx 2.00$). For each composition x the g value increases with decreasing temperature in contrast to the temperature-independent g values of both unoxidized Cu(PC) (Ref. 4) and of the molecular metal, Ni(PC)I.[2] This behavior results from strong exchange coupling between the two magnetic systems, and the temperature dependent g values may be described as the susceptibility weighted average of those of the individual components:[17]

$$g_{obs}(\phi, T) = f_{Cu}(T) g^{Cu}(\phi) + [1 - f_{\pi}(T)] g^{\pi} . \quad (3)$$

In Eq. (3), g^{π} is the isotropic g value of the π carriers, $g^{Cu}(\phi)$ is the Cu^{2+}-site orientation-dependent g value, ϕ is the angle between the external magnetic field and the crystal-needle axis, $f_{Cu}(T)$ is the fractional susceptibility of the Cu^{2+} spin system: $f_{Cu}(T) = \{\chi_{Cu}(T)/[\chi_{Cu}(T) + \chi_P]\}$, and $f_{\pi}(T) = 1 - f_{Cu}(T)$. Note particularly that $f_{Cu} \to 1$ as $T \to 0$ K, and that Eq. (3) thus predicts the $T = 0$ intercept to be $g^{Cu}(\phi)$ independent of x, in agreement with observation.

For samples of Cu_xNi_{1-x}(PC)I with $x \leq 0.50$, we have used the measured susceptibilities to calculate $f(T)$ within the temperature range, $20 \leq T \leq 300$ K and have calculated g^{Cu} and g^{π} by fitting experiment to Eq. (3). Static susceptibility data were not available for $x = 0.75$, but the results presented above indicate that it is appropriate to calculate $\chi_{Cu}(T)$ for this composition by assuming the Cu^{2+} spins contribute a Curie-Weiss susceptibility with $C = 0.75 C_0$, where C_0 is the value for Cu(PC)I, and $\Theta = -3$ K as interpolated from Fig. 4. The mobile charge carriers are assumed to exhibit a temperature-independent susceptibility similar to that observed for Ni(PC)I[2c], $\chi_p = 2 \times 10^{-4}$ emu K mol^{-1}.

As shown in Fig. 5 and in Fig. 5 of Ref. 3, for all x the temperature variation of the g values within the temperature range, $20 \leq T \leq 300$ K fits Eq. (3) well; in each case the fit yields $g_{\parallel}^{Cu} \approx 2.15$ (the $T = 0$ intercept, Fig. 5), $g_{\perp}^{Cu} \approx 2.04$ and $g^{\pi} \approx 2.00$. These results indicate that the Cu^{2+} and π carrier spin systems remain strongly coupled for all concentrations of Cu^{2+} sites studied, $x \geq 0.05$. However, it is interesting to note that the temperature dependences of $g_{\parallel}^{Cu}$ and $g_{\perp}^{Cu}$ for these alloys with $x \lesssim 0.75$

follow Eq. (3) well throughout the entire temperature range, $20 \leq T \leq 300$ K, in contrast to the case of pure Cu(PC)I where $g_{\perp}^{Cu}$ deviates from Eq. (3) below 100 K.[3]

Linewidth: temperature dependence

Figure 6 presents the temperature dependence for the linewidth at $g_{\parallel}$ for Cu_xNi_{1-x}(PC)I. As shown, the linewidth for each composition follows a temperature dependence having two separate regions; as x decreases the temperature at which the behavior changes also decreases. At high temperatures the linewidth decreases temperature; upon further cooling the linewidth increases. In addition, the data presented in Fig. 6 show that at any temperature, the linewidth decreases with increasing values of x.[19]

In the previous section, the EPR g value of Cu_xNi_{1-x}(PC)I has been analyzed in terms of strong exchange coupling between the local Cu^{2+} spins and the itinerant charge carriers. In such cases, the EPR linewidths will occur at the susceptibility weighted sum of the linewidths of the individual systems,[16]

$$\Delta_{obs} = f_{Cu}\Delta^{Cu} + f_{\pi}\Delta^{\pi} , \tag{4}$$

where f_{Cu} and f_{π} are the fractional susceptibilities of the component spin systems used in Eq. (3) and Δ^{Cu} and Δ^{π} and their intrinsic linewidths, defined as the half-width at half-height of the absorption signal. The fractional susceptibility of the Cu^{2+} spin systems at a given temperature increases with increasing x and extrapolates to unity at 0 K for all values of x [Eq. (3)]. Thus, the observed linewidth of Cu_xNi_{1-x}(PC)I is progressively dominated by the contribution of the local moments as the concentration of Cu^{2+} sites is increased, and for each x this is accentuated at low temperature; conversely, high temperatures and low values of x enhance the contribution of Δ^{π}. From the data taken upon cooling from room temperature (Fig. 6), it appears that Δ^{π} is moderately large and decreases upon cooling. It has been shown elsewhere[20] that under the high-temperature conditions of crystal growth employed, the π carriers of Ni(PC)I, which has no local spins, behave in a similar fashion. From the low-temperature data shown in Fig. 6, it appears that Δ^{Cu} increases upon cooling in a manner similar to that reported for Cu(PC)I. Thus, the temperature dependence of the linewidth of Cu_xNi_{1-x}(PC)I may be qualitatively understood: At higher temperatures, those compounds with the lowest Cu^{2+} concentration have linewidths that are dominated by the π carriers, and that decrease upon cooling. At low enough temperatures, the fractional susceptibility of the Cu^{2+} spins becomes dominant for all values of x, and the lines broaden upon cooling.

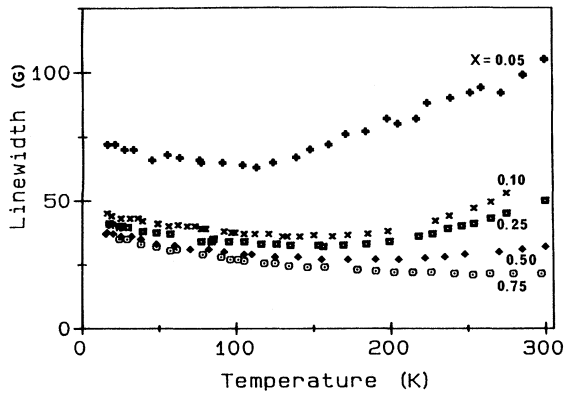

FIG. 6. Parallel component of the peak-to-peak EPR linewidths of Cu_xNi_{1-x}(PC)I plotted as a function of temperature.

Linewidth: angular dependence

The Cu_xNi_{1-x}(PC)I display an exchange-narrowed, Lorentzian signal at all values of x, with the linewidth at all temperatures increasing smoothly as x is lowered. This shape invariance provides qualitative evidence for a non-nearest-neighbor, indirect exchange between Cu^{2+} sites. A one-dimensional Cu^{2+} chain having only direct, near-neighbor interactions would display EPR signals that vary in both line shape and width as x decreases: dilution would destroy the exchange effects between neighboring sites and break the chain into progressively smaller magnetic segments, each having its own separate EPR properties, much as is observed for the insulating, deiodinated Cu_xNi_{1-x}(PC).

Quantitative analysis of the orientation dependence of the EPR linewidth of Cu_xNi_{1-x}(PC)I supports the presence of long-range, indirect Cu^{2+}-Cu^{2+} exchange. Studies of one-dimensional Cu^{2+} complexes[21] show that the interplay of strong dipolar and exchange interactions where the exchange frequency, ω_e, exceeds the Larmor frequency results in a narrowed EPR signal whose second moment has the dipolar dependence, $M_2 \propto (1+\cos^2\theta)$. We therefore use the expression $\Delta^{Cu} = \Delta_D(1+\cos^2\theta)$ in Eq. (3) to analyze the linewidth (derivative peak-to-peak) of the Cu^{2+} spins at ambient temperature.

$$\begin{aligned}\Delta(\theta) &= f_{\pi}\Delta^{\pi} + f_{Cu}[\Delta_D(1+\cos^2\theta)] \\ &\equiv \Delta_0 + \Delta_1(1+\cos^2\theta) ,\end{aligned} \tag{5a}$$

where the contribution of the angle-dependent term is set by the dipolar factor

$$\Delta_1 \equiv f_{Cu}\Delta_D , \tag{5b}$$

where Δ_D is the scalar factor determining the dipolar linewidth; unfortunately, the isotropic width, Δ_0, cannot be broken up into individual contributions. Figure 7 displays the angular dependence of the linewidths for single crystals of Cu_xNi_{1-x}(PC)I, with $x = 0.25$ and 0.10, taken at 20 K. A nonlinear least-squares fit of the data to Eq. (5a) is in good agreement with the experimental results (Fig. 7) and yields the following parameters: for $x = 0.25$, $\Delta_0 = 3(1)$ G, $\Delta_1 = 11(1)$ G; for $x = 0.10$, $\Delta_0 = 25(4)$ G, $\Delta_1 = 6(2)$ G. For $x > 0.25$, Δ_1 for $T = 20$ K was calculated directly, according to Eq. (5a): $\Delta_1 = [\Delta(\theta=0) - \Delta(\theta=\pi/2)]$. These two data sets are

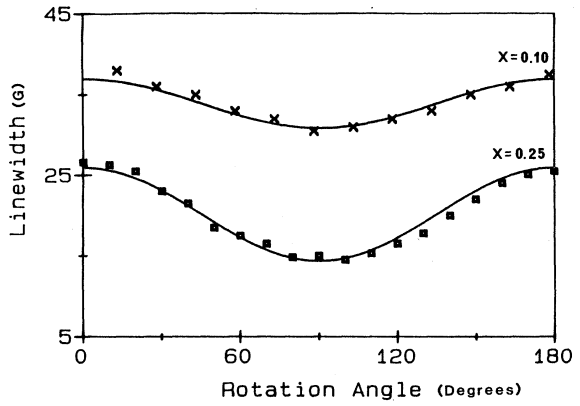

FIG. 7. Angular dependence of the peak-to-peak EPR linewidths of $Cu_{0.1}Ni_{0.9}$(PC)I and $Cu_{0.25}Ni_{0.75}$(PC)I taken at 20 K. The solid lines are the best fit of the data to Eq. (5a).

representative in that Δ_1 decreases but Δ_0 increases as x decreases. Because there is no obvious way to analyze Δ_0, we are forced to focus on Δ_1.

Figure 8 shows that the scalar dipolar factor, Δ_D (20 K), calculated from Δ_1 (Fig. 5) and Eq. (5b) decreases as x is lowered from $x=1.0$. As discussed above, the long-range dipolar interactions along the Cu^{2+} chain[21] varies roughly linearly with x, $M_2(x)=xM_2^0=x(8/3\sqrt{3})m_D$, where m_D is of the form

$$m_D=[3S(S+1)(g\beta)^3/r^6]\left[\sum_{n=1}^{\infty} n^{-6}\right]$$
$$=\tfrac{9}{4}[(g\beta)^3/r^6](1.0173)\ , \qquad (6)$$

where $r=c/2=3.195$ Å is the Cu-Cu spacing and $S=\frac{1}{2}$. In addition, studies of isolated local moments exchange coupled to itinerant spins[16] suggest that one should also allow for a second, temperature-dependent contribution to ω_e arising from the dynamic exchange between local and itinerant spins; $\omega_y \propto T$. We therefore attempt to describe the modulation of the Cu^{2+} spins by an effective exchange frequency of the function form, $\hbar\omega_e \sim J+\hbar\omega_y \sim k_B(a+bT)$. The first term, J is the rms value at a site for the sum of the direct and indirect quantum-mechanical exchange coupling between Cu^{2+} centers and thus in a mean-field model, $|\theta| \sim a/2\sqrt{2}$; bT represents the dynamical exchange between local and mobile spins. In the present case, we assume that long-range interactions are dominant, in which case the exchange should vary with composition as[13] $J \simeq a\sqrt{x}$. In accordance with this model, Δ_D of Eq. (6) becomes

$$\Delta_D=\frac{8}{3\sqrt{3}}\frac{xm_D}{\hbar\omega_e(x)}=\frac{8}{3\sqrt{3}}\frac{xm_D}{k_B(a\sqrt{x}+bt)}\ , \qquad (7)$$

where $m_d=1.58\times10^{-14}$ erg G, $a=7.1$ K, and $b=0.055$ was obtained from fits for $20 \lesssim T \lesssim 300$ K Cu(PC)I; there are no free parameters, the only variable being the occupation number of the Cu^{2+} sites, x. The values of Δ_D versus x at 20 K as calculated with Eq. (7) are plotted in Fig. 8 and are in reasonable agreement with the observed values of Δ_D.

EPR results: $T<20$ K

Figure 9 presents the temperature response of the normalized, low-temperature EPR linewidths ($T<20$ K) for $x=0.10,0.25,0.75$. As described above, the linewidths of these materials increase with decreasing temperature down to ca. $T_a \approx 20$ K(Fig. 6). Upon further cooling, Fig. 9, they deviate from this high-temperature behavior and remain constant down to a composition-dependent temperature, T_b, where a second, abrupt change is observed. As shown in Fig. 9, the EPR line of $Cu_{0.75}Ni_{0.25}$(PC)I rapidly broadens and becomes unobservable at $T_b \approx 8$ K in a manner similar to that seen for $x=1.0$, Cu(PC)I.[6] The EPR signal for a material with $0.10 \le x \le 0.50$ remains visible down to at least 2 K, but

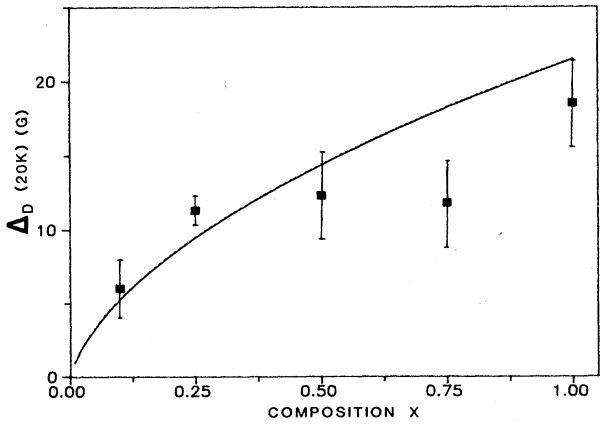

FIG. 8. Dipolar linewidth, Δ_D [Eq. (5)], of Cu_xNi_{1-x}(PC)I at 20 K ($x=0.10,0.25,0.50,0.75,1.0$) as a function of x. The solid line is obtained from Eq. (7) as described in the text.

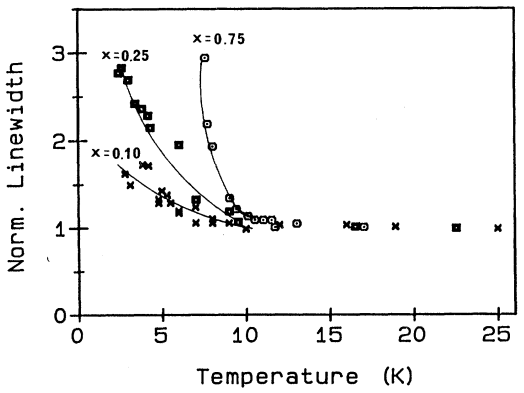

FIG. 9. Low-temperature EPR linewidth of Cu_xNi_{1-x}(PC)I ($x=0.10,0.25,0.75$), with H_0 parallel to the conducting chains. For each x the values are normalized to that at 30 K. Solid lines are to guide the eye.

the linewidths begin to increase at a temperature, T_b, which decreases as x decreases from 1.0. However, the rate at which the line broadens upon cooling below T_b, $(-d\Delta/dT)$, also decreases with x, and thus it is not possible to determine $T_b(x)$ accurately. By $x \sim 0.05$ anomalous linebroadening no longer is discernible (data not shown).

In addition to the weak deviations in the linewidth for $T \lesssim T_a$, there is a much more obvious deviation of the g values from the susceptibility-weighted average, Eq. (3). For $x \geq 0.25$, at $T_a \sim 17 \pm 3$ K the g values begin to increase above the value predicted by Eq. (3). The magnitude of this deviation depends on x, but because it begins gradually there is no clear dependence of the onset temperature on x. Figure 10 shows data for $x = 0.50$. By 2.4 K, $g_\parallel = 2.25$, strikingly far from that predicted from Eq. (3) ($g_\parallel^{\mathrm{Cu}} = 2.15$) and sharply greater than that previously observed for Cu(PC) in any environment. At still lower temperature lack of resolution in spectra of the powder samples employed prevents accurate measurement of $g_\parallel$. The discrepancies as measured at 2.4 K decrease with decreasing x: for $x = 0.50$, $g_\parallel^{\mathrm{Cu}} = 2.20$; for $x = 0.25$, $g_\parallel^{\mathrm{Cu}} = 2.17$; and for $x = 0.10$, $g_\parallel^{\mathrm{Cu}} = 2.16$. For $x \leq 0.10$, Eq. (3) is followed accurately down to 5 K at least. Thus, as with the EPR linewidths, the extent of the deviation from the high-temperature prediction is correlated with the Cu content of these materials.

Prompted by observations in the related system, Cu(TATBP)I, we performed EPR measurements at a higher magnetic field (microwave frequency, 35 GHz). The g values at convenient selected temperatures in the high-temperature regime (270 K, 100 K) match to those at X-band frequencies. However, in the low-temperature regime they are not the same. As illustrated in Fig. 10, the Q-band values do not show a sharp rise seen at X-band values, but remain at $g \sim 2.18$ down to $T \sim 2.13$ K. Thus, the anomalous g shift seen at the X band is quenched at higher observing fields, and the electronic structure itself, as reflected in $g_\parallel$, is a function of the applied field.

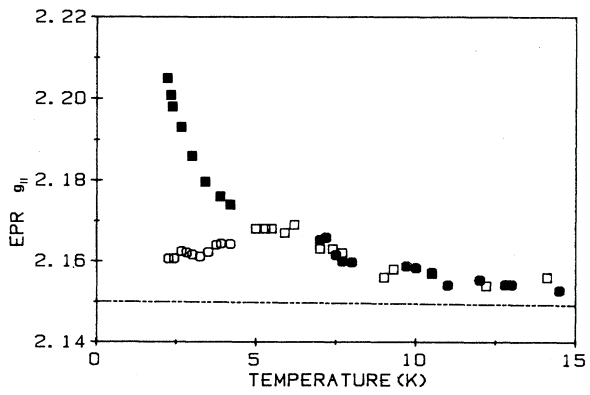

FIG. 10. Low-temperature behavior of $g_\parallel$ for $Cu_{0.5}Ni_{0.5}$(PC)I: □, single crystal at X band; ■, powder at X band; and ○, powder at Q band. Single-crystal data (●) for Cu(PC)I also are shown.

Conductivity in Cu_xNi_{1-x}(PC)I

In Fig. 11, we present a log-log plot of the four-probe and microwave conductivity as a function of temperatures for single crystals of Cu_xNi_{1-x}(PC)I. All the alloys behave similarly: The conductivity is metallic at room temperature, reaches a maximum as the temperature is progressively decreased and rapidly drops upon further cooling. As shown for $x = 1$, the four-probe[22] and microwave measurements (normalized at $T = 300$ K) show broad agreement down to ~ 10 K, indicating that the maximum at ~ 90 K is an intrinsic property and not caused by strains from the contacts. Figure 11 further shows that as x decreases: (1) the absolute microwave conductivity of Cu_xNi_{1-x}(PC)I increases; (2) the conductivity maximum shifts to lower temperature; and (3) the fall at lower temperatures becomes less steep. Four-probe measurements of $\sigma(T)$ to low temperature for Cu_xNi_{1-x}(PC)I, $x < 1$, is difficult because the crystals are very fragile. However, one crystal each of Cu_xNi_{1-x}(PC)I, $x = 0.75, 0.50, 0.25$, has been successfully cycled throughout the entire temperature range, 5–300 K (data not shown) with similar results.

Significant discrepancy between the two techniques is observed at lower temperatures. Figure 11 also shows that for $x = 1$ as the crystal is cooled below $T_c \sim 8$ K, approximately the transition temperature, T_b, seen in the EPR measurements, the microwave conductivity becomes constant and is *enhanced* in comparison to the dc conductivity. The data for the three alloys further suggests that T_c decreases with x. In this low-temperature range the limited four-probe data for all x follows that for $x = 1$ in that σ smoothly decreases down to the lowest

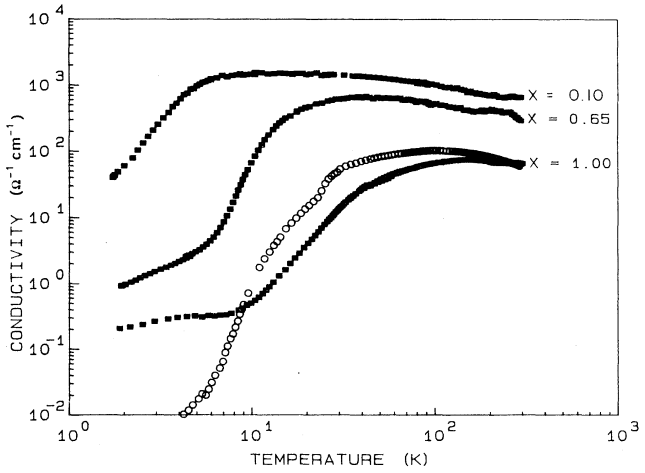

FIG. 11. Temperature dependence of the four-probe (○) and microwave (■) conductivity (Ω^{-1} cm^{-1}) of Cu_xNi_{1-x}(PC)I taken along their needle axes. The maxima appearing around 60 K are reversible upon a complete temperature cycle; the break in the curve for $x = 1.0$ at $T \sim 20$–30 K is an artifact.

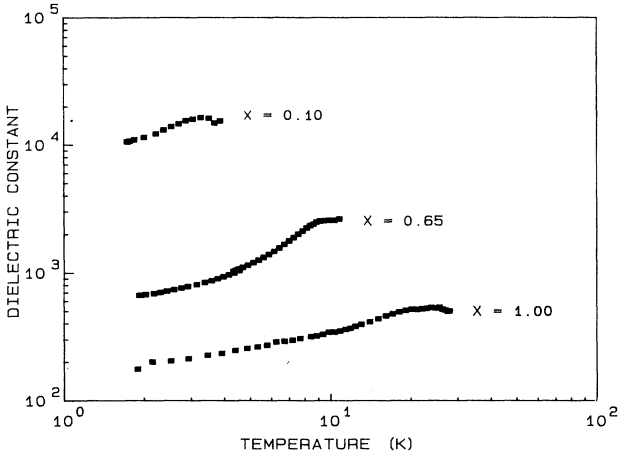

FIG. 12. Dielectric constant of Cu_xNi_{1-x}(PC)I for $x=0.10$, 0.75, and 1.00.

temperature accessible, $T\sim 5$ K, and does not show such a change in slope.

To understand the conductivity, one has also to consider the behavior of the dielectric constant. In Fig. 12, we present the microwave dielectric constant as a function of temperature for the same compounds; because the conductivity is relatively high, results can be obtained only at low temperatures. The dielectric constant is quite high and increases with temperature; however, it is a decreasing function of the Cu^{2+} concentration. These results are extremely surprising because they imply an important coupling between the magnetic and the dielectric properties of the structure.

DISCUSSION

The results presented here have shown that the Cu_xNi_{1-x}(PC)I are homogeneous alloys of the molecular metals, Cu(PC)I and Ni(PC)I. These materials possess charge carriers associated with the π orbitals of the PC ring and have Cu centers that retain their paramagnetic ($S=\frac{1}{2}$) +2 oxidation state.

The EPR signal of Cu_xNi_{1-x}(PC)I consists of a single line whose temperature-dependent g value arises from strong exchange coupling between local moments and itinerant carriers. Its width displays the characteristic anisotropy of strongly exchange-narrowed dipolar interactions within a one-dimensional chain, which demonstrates that the Cu^{2+} sites dominate the EPR properties of these materials. As the concentration of Cu^{2+} sites is systematically lowered, the EPR signals of Cu_xNi_{1-x}(PC)I remain homogeneous and characteristic of exchange-narrowed dipolar interactions down to low values of x, which behavior suggests the presence of long-range exchange interactions between distant Cu^{2+} sites. This interaction is believed to be mediated through the itinerant charge carriers because such behavior is observed only for the conductive Cu_xNi_{1-x}(PC)I and not the deiodinated Cu_xNi_{1-x}(PC), whose EPR spectra exhibit a complicated composition dependence, as expected for near-neighbor exchange. Furthermore, the existence of long-range Cu-Cu interactions in the Cu_xNi_{1-x}(PC)I is consistent with the composition dependence of their linewidths, Eq. (7), as previously observed for atomic spin glasses.

As an apparent result of this unusual long-range coupling between Cu^{2+} spins, the EPR signal of Cu_xNi_{1-x}(PC)I exhibits a series of composition-dependent, low-temperature anomalies qualitatively similar to those observed for Cu(PC)I, $x=1.0$. At $T_a\approx 20$ K, the g values of those compounds having $x\geq 0.25$ begin to rise above the values predicted from the susceptibility-weighted behavior of coupled local and itinerant spins. The X-band g values reached at $T<2$ K are far greater than that extrapolated from high-temperature measurements, and far higher than have ever been reported for Cu(PC) under any circumstances. However, the large g shifts are field dependent, being quenched at Q-band frequencies. This suggests that the Cu_xNi_{1-x}(PC)I are not undergoing a spin-Peierls (SP) transition.[23] The X-band EPR signal disappears at temperatures below a SP transition; it remains visible in measurements at very high observing fields and is found to show unusual g shifts. This is in contrast to the report here of large X-band g shifts that are quenched upon increasing the observing field from $\sim 0.3T$ (X band) to $\sim 1.2T$ (Q band).

For $x\geq 0.1$, the $g_{\parallel}$ linewidth increases as the temperature is lowered to T_a, and are temperature independent upon further cooling to T_b; at still lower temperatures the linewidths begin to broaden sharply, but the g value continues to increase smoothly. The EPR signal of $Cu_{0.75}Ni_{0.25}$(PC)I becomes unobservably broad at $T_b\sim 8$ K in a manner identical to that seen for Cu(PC)I. For compounds having lower percentage of Cu^{2+} spins in the metal-ion chain the signal broadens below T_b, but remains observable. As x decreases, T_b decreases and the broadening ($-d\Delta/dT$) is progressively reduced. In the limit of high dilution of Cu^{2+} sites, $x\lesssim 0.05$, the T_b anomaly disappears.

Although the conductivity is associated with π carriers on the macrocycle, nevertheless, its dependence on the composition x clearly shows that σ is controlled by interactions with the $S=\frac{1}{2}$ local moments on Cu^{2+}. The exact nature of the conductivity maximum is not fully understood, but it is not believed to be associated with a metal-insulator or semiconductor transition since for Cu(PC)I the thermopower measurement[3] indicates a metallic behavior down to 10 K. The rapid drop of the conductivity may thus be qualitatively associated with magnetic scattering of the carriers—an independent-Kondo-impurity model.[24,25] As the temperature is decreased, the magnetic local moments become more efficient as scattering centers for free carriers and a maximum is observed in the conductivity data. An external magnetic field should partially freeze the local moments and thus reduce the scattering rate of the itinerant carriers: indeed, as shown elsewhere this results in a positive magnetoconductivity.[26] Unfortunately, no exact model may be found in the literature for such a one-dimensional Kondo system. Furthermore, the results are not in quantitative agreement with the conventional three-

dimensional Kondo model; the temperature dependence is not observed and the drop in conductivity of over three orders of magnitude below the maximum is much larger than the value generally obtained in the three-dimensional Kondo system (10%).[24] These discrepancies might be attributable to the low dimensionality of these compounds: scattering and localization effects are expected to be more dramatic in one dimension.

The sharp departure between four-probe and microwave measurement at low temperatures occurs approximately at the same temperature where the EPR linewidth suddenly increases: $T_c \sim T_b$. At these temperatures the EPR signal is dominated by the Cu^{2+} local moments [$f(T) \rightarrow 1$], an observation that reinforces the proposition that the frequency dependence of the conductivity in this regime is also related to the local moments. The presence of important coupling between magnetic and dielectric properties is confirmed by the surprising dependence of the dielectric constant on the Cu^{2+} concentration.

ACKNOWLEDGMENTS

This work has been supported by the Solid State Chemistry Program of the National Science Foundation (NSF) (Grant No. DMR 85-19233; B.M.H.) and by the Northwestern University Materials Research Center under the National Science Foundation Materials Research Laboratories Program (NSF-MRL) (Contract No. DMR 85-20280, B.M.H. and J.A.I.) and by the Natural Sciences and Engineering Research Council, Canada (NSERC) and FCAR (M.P.).

[1]For a review on molecular metals, see for example, (a) *Proceedings of the Internal Conference on the Physics and Chemistry of Low Dimensional Synthetic Metals, Crystals* [Mol. Cryst. Liq. Cryst. **119-120**, (1985)]; edited by C. Pecile, G. Zerbi, R. Bozio, and A. Girlando. (b) J. M. Williams, M. A. Beno, H. H. Wang, P. C. W. Leung, T. J. Emge, U. Geiser, and K. D. Carlson, Acc. Chem. Res. **18**, 261 (1985). (c) F. Wudl, *ibid.* **17**, 227 (1984). (d) R. L. Greene, Science (Washington, D.C.) **226**, 651 (1984).

[2](a) C. J. Schramm, R. P. Scaringe, D. R. Stokakovic, B. M. Hoffman, J. A. Ibers, and T. J. Marks, J. Am. Chem. Soc. **102**, 6702 (1980). (b) J. Martinsen, R. I. Greene, S. M. Palmer, and B. M. Hoffman, *ibid.* **105**, 677 (1983). (c) J. Martinsen, S. M. Palmer, J. Tanaka, R. L. Greene, and B. M. Hoffman, Phys. Rev. B **30**, 6269 (1984).

[3]M. Y. Ogawa, J. Martinsen, S. M. Palmer, J. L. Stanton, J. Tanaka, R. L. Greene, B. M. Hoffman, and J. A. Ibers. J. Am. Chem. Soc. **109**, 1115 (1987).

[4]Soonchil Lee, M. Yudkowsky, W. P. Halperin, M. Y. Ogawa, and B. M. Hoffman, Phys. Rev. B **35**, 5003 (1987).

[5]K. K. Liou, M. Y. Ogawa, T. P. Newcomb, G. Quirion, M. Poirier, B. M. Hoffman, and J. A. Ibers (unpublished).

[6](a) M. Y. Ogawa, B. M. Hoffman, S. Lee, M. Yudkowsky, and W. P. Halperin, Phys. Rev. Lett. **57**, 1177 (1986); (b) M. Y. Ogawa, S. M. Palmer, J. Martinsen, J. L. Stanton, B. M. Hoffman, J. A. Ibers, S. Lee, M. Yudkowsky, and W. P. Halperin, Synth. Met. **19**, 781 (1987).

[7](a) G. Quirion, M. Poirier, M. Y. Ogawa, and B. M. Hoffman, Solid State Commun. **64**, 613 (1987); (b) G. Quirion, M. Poirier, K. K. Liou, M. Y. Ogawa, and B. M. Hoffman, Phys. Rev. B **37**, 4272 (1988).

[8]D. F. Shriver and J. B. R. Dunn, Appl. Spectrosc. **28**, 319 (1974).

[9](a) M. J. Nilges, Ph.D. thesis, University of Illinois, Urbana, Illinois, 1981; (b) T. E. Altman, *ibid.* 1981; (c) A. M. Marice, *ibid.* 1982; (d) E. P. Duliba, *ibid.* 1983.

[10]L. I. Burovov and I. Schogolev, Prib. Tekh. Eskp. **2**, 171 (1971).

[11](a) R. C. Teitelbaum, S. L. Ruby, and T. J. Marks, J. Am. Chem. Soc. **100**, 3215 (1978); (b) **102**, 3322 (1980).

[12]S. E. Harrison and J. M. Assour, J. Chem. Phys. **40**, 365 (1964).

[13]A. Abragam, *Principles of Nuclear Magnetism* (Oxford University Press, Oxford, 1961).

[14]J. R. Pilbrow, A. D. Toy, and T. D. Smith, J. Chem. Soc. A **6**, 1029 (1969).

[15]J. S. Smart, *Effective Field Theories of Magnetism* (Saunders, Philadelphia, 1966).

[16]S. E. Barnes, Adv. Phys. **30**, 801 (1980); **30**, 938 (1980).

[17]P. Gans, G. Buisson, E. Duee, J.-C. Marchon, B. S. Erler, W. F. Scholz, and C. A. Reed, J. Am. Chem. Soc. **108**, 1223 (1986).

[18]The magnitude of Θ_{ind} can be interpreted through a simple mean-field approximation (Ref. 19) to give a value for $J_{d\text{-}\pi}$ that is reasonably consistent with those seen in metalloporphyrins. However, more detailed treatments are required (e.g., Ref. 16), as the simplest mean-field treatments would require $\Theta_{ind} > 0$, contrary to observation.

[19](a) L. Alcacer and A. H. Maki, J. Phys. Chem. **80**, 1912 (1976); (b) Y. Tomkiewicz, A. R. Taranko, and J. B. Torrance, Phys. Rev. B **15**, 1017 (1977). (c) E. Conwell, *ibid.* **22**, 3107 (1980).

[20]S. M. Palmer, Ph.D. thesis, Northwestern University, 1985.

[21](a) Z. G. Soos, T. Z. Huang, J. S. Valentine, and R. C. Hughes, Phys. Rev. B **8**, 993 (1973); (b) K. T. McGregor and Z. G. Soos, J. Chem. Phys. **64**, 2506 (1976).

[22]The conductivity of crystals with $x = 1$ prepared at the higher temperatures employed here differ in detail from that reported earlier (Ref. 3) for Cu(PC)I prepared at lower temperatures. The room-temperature conductivity not only is slightly lower [(1.5–2)-fold], but they show a conductivity maximum at $T_m \sim 90$ K, rather than at 20–30 K. We will discuss investigations of this phenomenon elsewhere. However, we note that the results reported here have been reproduced with many crystals from many preparations and that for *all* magnetic measurements, the properties of *all* preparations of Cu(PC)I are indistinguishable.

[23]T. W. Hijmans and W. P. Beyermann, Phys. Rev. Lett. **58**, 2351 (1987).

[24]G. Grüner and A. Zawadowski, Rep. Prog. Phys. **37**, 1497 (1974).

[25]H. Keiter and G. Morandi, Phys. Rep. **109**, 227 (1984).

[26]G. Quirion, M. Poirier, K. K. Liou, M. Y. Ogawa, and B. M. Hoffman (unpublished).